American Mineralogist, Volume 67, pages 244–250, 1982

Representation of compositions in complex titanian spinels and application to the De Beers kimberlite

JILL DILL PASTERIS

Department of Earth and Planetary Sciences and
McDonnell Center for the Space Sciences
Washington University, St. Louis, Missouri 63130

Abstract

Irvine's (1965, 1967) papers on the use of spinels as petrogenetic indicator phases have made petrologists more aware of the thermodynamic approach to evaluating spinel compositions. The six-endmember spinel prism plot (Irvine, 1965) and two-parameter projections of it are now common in the literature. However, various researchers have chosen to give different meanings to the established parameters.

Since Irvine's papers originally were published, a large body of data has accumulated on kimberlitic spinels. The latter tend to be high in Ti, an element not considered in the original spinel prism plot. Attempts have been presented in the literature for direct adaptation of the prism plot by replacing ferric iron endmembers with titanian ones. However, the unique structural formula of titanian spinels changes the configuration of the spinel prism. More importantly, commonly used ratio plots of the form Cr/(Cr+Al) *vs.* $Fe^{2+}/(Fe^{2+}+Mg)$ can be misleading for titanian spinels. If two-parameter plots are desired, it is suggested that those of the form Cr *vs.* Fe^{2+} be among the diagrams used to depict compositional differences among and fractionation trends in kimberlitic and other titanian spinels. Such diagrams have been used successfully to distinguish suites of spinels from several kimberlite intrusions in the De Beers Pipe, South Africa.

Introduction

Since the appearance of Irvine's (1965) article on chromian spinel compositions as petrogenetic indicators, petrologists have examined more carefully the compositions, zoning trends, and mineralogic associations of spinels in mafic and ultramafic rocks. In addition to the useful features presented by Irvine (1965), the following factors make spinel phases particularly important in kimberlites: (1) spinels are among the few phases not appreciably altered in most kimberlites; and (2) they have preserved a compositional zonation indicative of changing conditions in the melt. Analyses are now available for kimberlitic spinels from several regions throughout the world (*e.g.*, Haggerty, 1975; Boctor and Meyer, 1979; Elthon and Ridley, 1979; Mitchell, 1978a, 1978b, 1979; Mitchell and Meyer, 1980; Pasteris, 1980).

The purpose of this paper is not to review in detail the compositional patterns of kimberlitic spinels, but rather to discuss and evaluate means of plotting spinel compositions for effective intercomparisons among pipes. The distinctive compositional patterns in kimberlitic spinels, especially the increase in Ti from core to rim in the grains, call for a re-evaluation of plotting techniques. In particular, cation-cation diagrams appear to be a useful empirical method for enhancing spinel compositional differences, as demonstrated for the De Beers kimberlite pipe (Pasteris, 1980).

Plotting techniques for spinel compositions

In the course of a study of the spinel phases of the De Beers kimberlite (Kimberley, South Africa), compositional data on spinels from this and about fifteen other kimberlites were compiled (Pasteris, 1980). Several types of graphs were compared to determine which are the most effective in depicting differentiation trends in a given kimberlite and compositional differences between kimberlites. In particular, the relative merits of spinel prism diagrams (*e.g.*, Irvine, 1965), cation ratio plots (*e.g.*, Arculus, 1974; Ridley, 1977; Haggerty, 1979; Boctor and Meyer, 1979), and pure cation plots (Pasteris, 1980) were examined. The results of this

0003–004X/82/0304–0244$02.00

comparison have general petrologic application, in particular to basalts and kimberlites showing Ti-enrichment in their spinels.

The spinel prism and its projections

Compositionally spinel analyses from igneous rocks usually can be treated in terms of eight important endmember components (Table 1a). In order to represent all possible spinel endmembers, Datta and Roy (1967) presented the following structural formula for spinels, which designates octahedral and tetrahedral site occupancy: $(B_xA_{1-x})^{IV}$-$(A_xB_{2-x})^{VI}O_4$. This formula reduces to the familiar expression AB_2O_4 and also indicates the full range of structural types intermediate between inverse spinel (x=1) and normal spinel (x=0) endmembers. In this paper, the further distinction will be made between 2–4 spinels, of the form $X_2^{2+}Y^{4+}O_4$, and 2–3 spinels, of the form $X^{2+}Y_2^{3+}O_4$.

Stevens (1944) suggested plotting six selected endmembers in a triangular prism (Johnston method; Figure 1, this paper), a method adopted by many petrologists. According to a convention to be examined in this manuscript, titanian apical endmembers typically have been chosen to represent kimberlitic spinel compositions in the prism.

Irvine's (1965) geometric projection methods for the spinel prism account for atomic proportions of Fe^{3+}, Al, and Cr, but not for Ti. Other petrologists have extended Irvine's approach to Ti-bearing spinels, but in addition, some potentially misleading practices have appeared in the literature: (1) plotting *total* Fe, even though only Fe^{2+} endmembers exist on the diagram; (2) plotting *weight* percent oxides, which do not clearly reflect cation occupancy and substitution; (3) using the cation ratio Ti/(Ti+Cr+Al), which neglects the special stoichiometry of titanian spinels; and (4) using a norm-type calculation to derive percentages of endmember components (*e.g.*, Mitchell, 1978a, 1978b, 1979; El Goresy, 1976; Haggerty, 1976; Boctor and Meyer, 1979).

Table 1. Spinel stoichiometries

1A Common Spinel Endmembers

$FeCr_2O_4$	(chromite)	Fe_3O_4	(magnetite)
$MgCr_2O_4$	(picrochromite)	$MgFe_2O_4$	(magnesioferrite)
$FeAl_2O_4$	(hercynite)	Fe_2TiO_4	(ulvospinel)
$MgAl_2O_4$	(spinel)	Mg_2TiO_4	(magnesium titanate)

1B Misleading Nature of Cr/(Cr + Al) Ratios

For CCA = 0.5, the following are only two possible cases for non-titanian spinels: where CCA = Cr/(Cr + Al)

CCA = 0.3/(0.3 + 0.3)	Fe^{3+} = 1.4	ΣY^{3+} = 2
CCA = 0.8/(0.8 + 0.8)	Fe^{3+} = 0.4	

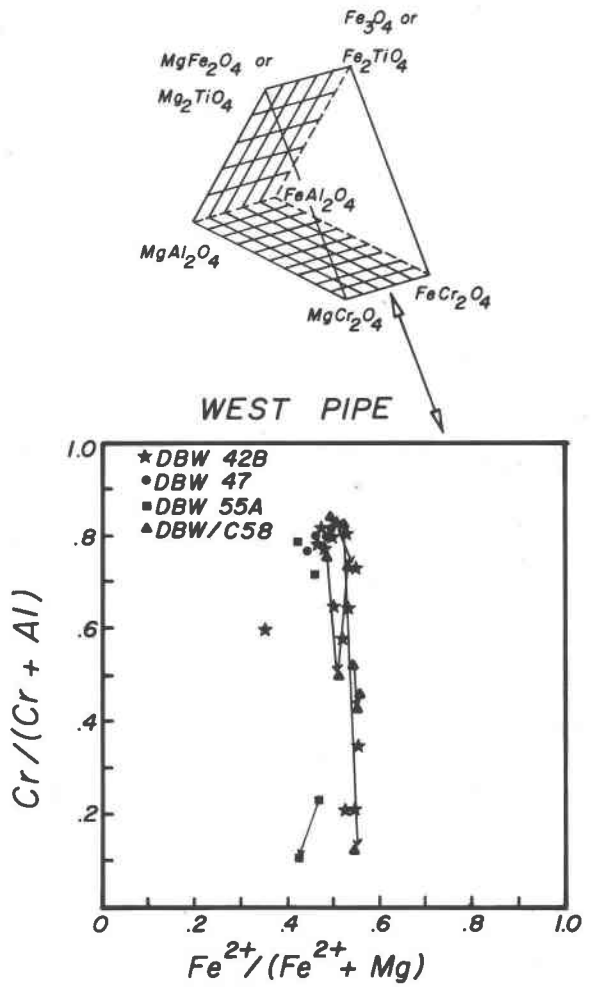

Fig. 1. Spinels from the West Pipe of the De Beers Kimberlite Pipe, Kimberley, South Africa. CCA *vs.* FFM plot; projection onto the base of the spinel prism. Each symbol represents a rock sample from a different depth in the pipe

It often is difficult to envision in three-dimensional space the compositional relationships depicted by the spinel prism. However, as illustrated by Irvine (1965) and Haggerty (1976), the data lend themselves to projection onto the faces of the prism. One common projection is onto the bottom rectangle, plotting the ratio Cr/(Cr+Al) against Fe^{2+}/(Fe^{2+}+Mg) (abbreviated CCA *vs.* FFM; Figure 1, this paper). The silicate-spinel reactions examined by Irvine (1965, 1967) and Jackson (1969) clearly

indicate the usefulness of such ratio plots. However, for reasons to be discussed in the following sections, this plotting technique should be modified before applying it to 2–4 spinels, including those containing Ti.

Ratio plots

The spinel prism diagram and its projections (cation ratio plots) originally were applied to the most common six spinel endmembers, those of the 2–3 type, having the form $X^{2+}Y_2^{3+}O_4$. Although ratio plots are useful, they tend to obscure certain trends in which 2–4 spinel components are involved. On a cation ratio plot in which divalent cations (X) other than Fe^{2+} and Mg are of negligible importance, one might assume that $(Fe^{2+}/\Sigma X)\sim$ "Fe^{2+} per 4 oxygens." However, ulvöspinel and magnesium titanate (2–4 spinels) have the form X_2YO_4, where Y = Ti. Thus, $\Sigma X = 2$ for the titanian endmembers rather than 1 as in the other spinels; for spinels with a titanium component, $(Fe^{2+}+Mg)$ does not equal 1, but rather is approximately (1+Ti) (only approximately, due to almost negligible amounts of Ni, Ca, Mn, and Si). The ratio $Fe^{2+}/(Fe^{2+}+Mg)$ and the term "Fe^{2+} per 4 oxygens" may differ greatly in the presence of a high ulvöspinel content (see Table 2). This partly explains the effect seen in CCA *vs.* FFM graphs in which spinels of widely varying CCA ratios have an almost constant FFM ratio (Fig. 1). The apparent Fe–Mg constancy is also seen in spinel prism plots and has led some workers to suggest there is little differentiation in kimberlitic spinels (*e.g.*, Mitchell and Meyer, 1980). Haggerty (1979) alluded to the disruptive effects of Ti on the Fe *vs.* Mg plots he found useful for characterizing spinels from high-pressure regimes.

Table 2. Effect of Ti on $Fe^{2+}/(Fe^{2+}+Mg)$ ratios in spinels

$Fe^{2+}/(Fe^{2+}+Mg)$: where $Fe^{2+}+Mg \neq 1$

$Fe^{2+}+Mg = 1+Ti$

Examine $\Sigma X^{2+} = 1.3$ and 1.45:

Fe^{2+}: for $\Sigma X^{2+} = 1.3$, $Fe^{2+}/(Fe^{2+}+Mg)=$	for $\Sigma X^{2+} = 1.3$, Mg =	for $\Sigma X^{2+} = 1.45$, $Fe^{2+}/(Fe^{2+}+Mg)=$	for $\Sigma X^{2+} = 1.45$ Mg=
0.1	0.077	1.2	0.069	1.35
0.2	0.154	1.1	0.138	1.25
0.3	0.231	1.0	0.207	1.15
0.4	0.308	0.9	0.276	1.05
0.5	0.385	0.8	0.380	0.95
0.6	0.462	0.7	0.414	0.85
0.7	0.538	0.6	0.483	0.75
0.8	0.615	0.5	0.552	0.65
0.9	0.692	0.4	0.621	0.55
1.0	0.769	0.3	0.690	0.45
1.1	0.846	0.2	0.759	0.35
1.2	0.923	0.1	0.828	0.25
1.3	1.000	0.0	0.897	0.15
1.45	-----	---	1.000	0.00

As indicated in the equations above, the greater the Ti-content of the spinel, the larger the sum of Fe(II) and Mg, and the greater the difference between Fe(II) and the ratio Fe(II)/Fe(II) + Mg. During crystal fractionation, the Fe(II)-content of spinel usually rises, as does the Ti-content in many cases. The effect of the latter is to maintain a higher Mg-content than would have been the case if Ti had remained constant, and only Fe(II) had risen.

The ratio Cr/(Cr+Al) is also misleading if other components such as Fe^{3+} are present. Although magnetite has the same XY_2O_4 stoichiometry as chromites and aluminates, a disregard for the Fe^{3+} component could lead one to conclude that two spinels have the same composition, when they are actually distinctly different in chemistry and crystallization conditions. As shown in Table 1b, spinels with very different Fe^{3+} contents can have exactly the same CCA ratios. This could result in the labeling as pleonastes those spinels with very low CCA ratios, even though their *absolute* concentrations of Al (as well as of Cr) are extremely low, as in aluminous magnetites. Jackson (1969) and Roeder *et al.* (1979) addressed this complication in their olivine–spinel geothermometers. Jackson (1969) projected data points onto planes *within* the spinel prism and used ratios of the form $Cr/(Cr+Al+Fe^{3+})$ as the ordinate. Roeder *et al.* (1979), on the other hand, used the ratio Cr/(Cr+Al) as one axis on their diagram, but kept the atomic ratio of Fe^{3+} constant, thus eliminating one compositional variable.

The CCA ratio also is affected by the presence of Ti, in particular because of the X_2YO_4 stoichiometry of 2–4 spinels. Therefore, it is possible for spinels with different Fe^{3+} and Ti contents to plot at almost the same CCA ratio or as a range of CCA ratios not representative of variations in bulk mineral compositions. Distortions are particularly evident toward the ends of differentiation trends because of late-stage enrichment in Fe^{3+} and/or Ti. It appears that this may account for the compositional patterns seen in many spinel suites from kimberlites (see Fig. 1, Table 2).

It seems clear that the CCA *vs.* FFM ratio plots employed for many suites of igneous and metamorphic spinels may be confusing when improperly applied to kimberlitic and other titanian spinels. A more complex thermodynamic formulation than that considered by Irvine (1965), Jackson (1969), and Roeder *et al.* (1979) could be written which accounts for Ti as well as Cr, Al, and Fe^{3+} (*cf.* Rawson and Irvine, 1980). However, this would serve to increase the number of compositional variables, making the ratio plots less straight forward. Pasteris (1980), for instance, employed the

plot $Fe^{3+}/(Fe^{3+}+2Ti+Cr+Al)$ *vs.* $Fe^{2+}/(Fe^{2+}+Mg)$ on kimberlitic spinels, but found that otherwise detectable distinctions among spinel suites were obscured.

Thermodynamic versus empirical constraints

The considerations involved in choosing a plotting method are both theoretical and empirical. From a theoretical viewpoint, the thermodynamics of the spinel system are important. Compositional diagrams at least should properly represent known cation exchange equilibria among the phases. However, the spinel system is very complex. Within the eight-component system under consideration, non-Vegardian behavior occurs along many joins, several solvi exist at magmatic temperatures (*e.g.*, Muan *et al.* 1972), and defect solid solution and/or the presence of Ti^{3+} and Cr^{2+} are possible (*e.g.*, Mao and Bell, 1974; Haggerty, 1979). These complications make the development of a general thermodynamic treatment difficult. Until a widely accepted model is developed to account for spinel systematics, procedures applicable to simple subsystems should be applied with caution to the extended spinel system. This is particularly true when one attempts to represent accurately on a two-parameter plot the behavior of a complex, non-ideal multicomponent system.

The thrust of this paper is essentially empirical. From that viewpoint, the basic need of those attempting to evaluate spinel data from kimberlites is a means of comparing compositions of spinels (1) from different pipes (as a reflection of different kimberlite bulk compositions and fractionation trends) and (2) from within the same pipe (as a reflection of fractionation).

The question posed by the petrologist concerns how the spinel compositions relate to silicate–oxide–melt equilibria. The complexities of spinels strongly affect their compositional response during crystallization. However, within certain subsystems of the spinel system and given certain known constraints on factors such as oxygen fugacity and temperature, successful estimates of conditions of crystallization and re-equilibration between spinel and silicate phases have been made (*e.g.*, Medaris, 1975; Evans and Frost, 1975).

Obviously one does not cease to plot spinel compositions while waiting for the thermodynamics to be worked out. However, in addition to the continued but more cautious use of ratio plots, it seems appropriate that certain compositional plots for spinels could be selected empirically and applied usefully, as long as their interpretations reflect their origin. With regard to plots of element partitioning among phases, such an empirical approach on occasion has aided understanding of reaction equilibria.

Cation-cation plots

In this author's experience, Cr *vs.* Fe^{2+} cation–cation plots have proved very useful in distinguishing compositional patterns in spinels from kimberlites (Fig. 2). The well documented sensitivity of spinel compositions to conditions in the melt and the regularity of the above patterns suggest that

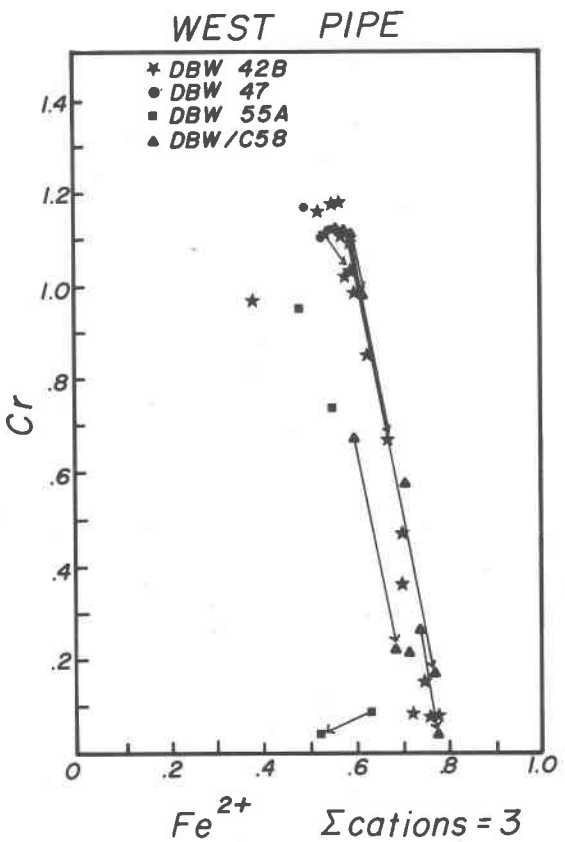

Fig. 2. Spinels from the West Pipe of the De Beers Kimberlite. Same data set and symbols as in Fig. 1, but plotted on the cation–cation diagram Cr *vs* Fe^{2+}. Compare the cation–cation plot (Fig. 2) to the analogous ratio plot (Fig. 1) for the same spinel analyses. In the cation graph, the differentiation interval (ΔFe^{2+}) is $0.38 \rightarrow 0.77 = 0.39$ compared to the interval $0.35 \rightarrow 0.56 = 0.21$ for the ratio plot. The vertical range of the data in the cation plot is $0.04 \rightarrow 1.18 = 1.14$, rather than only $0.11 \rightarrow 0.85 = 0.74$ on the ratio graph. The cation graphing method spreads the data over a larger interval and also resolves subtle differences among samples. (A plot of $Fe_{tot}/(Fe_{tot} + Mg)$ for the West Pipe looks similar to Fig. 1, except that the data are all shifted to the right, and there is even less resolution between the samples.)

such cation–cation plots may reflect crystal–liquid partition coefficients and changes in magma composition (Navrotsky, personal communication; *cf.* Haggerty, 1979, and numerous references on lunar spinels, such as El Goresy, 1976).

In cation–cation plots, the cation values are normalized in that they sum to 3 for a spinel phase of AB_2O_4 stoichiometry. Although the FFM ratio $Fe^{2+}/(Fe^{2+}+Mg)$ cannot exceed 1, cation site occupancy for Fe^{2+} may be as high as 2 (*e.g.*, Fe_2TiO_4). Therefore, relationships are much less compressed on a diagram using Fe^{2+}as a variable than on an FFM ratio plot (compare Figs. 1 and 2). Table 2 exemplifies how the same FFM ratio may arise in two compositionally different situations which are distinguished by their cation values. The following example from the De Beers kimberlite demonstrates the usefulness of plotting Cr *vs.* Fe^{2+} to represent titanian spinels.

Application to the De Beers kimberlite

Several (3 to 5) intrusion episodes are represented in the De Beers kimberlite diatreme. An exact number and chronological order of the intrusions are suggested by field evidence, but petrologic confirmation of the relationships was sought. Much of the silicate material in the kimberlite has been replaced by serpentine or carbonate, but the opaque oxide phases appear much less altered. Because strong compositional zoning exists in many spinel grains from the De Beers kimberlite, this phase was analyzed as a means of more clearly distinguishing the number and order of the intrusions.

A CCA *vs.* FFM plot ($Cr/Cr+Al$ *vs.* $Fe^{2+}/Fe^{2+}+Mg$) for the spinels from one region of the kimberlite pipe appears in Figure 1. It is obvious that spinels of a wide range in CCA values have a very narrow range in FFM values. This suggests that the composition of a co-precipitating silicate phase may be buffering the composition of the spinels, in analogy to the situation described by Irvine's (1965) equipotential surfaces for spinel in the presence of olivine.

Three reasons come to mind why the almost vertical slope on the above graph is not a direct function of an equipotential surface in the sense defined by Irvine (1965). (1) The textures and compositional ranges of many kimberlitic spinels suggest that they formed over a wide range of temperatures. (2) Because of the altered and brecciated nature of kimberlite, it is not clear that any particular silicate phase (especially the same silicate phase) is co-precipitating continuously with the spinels. (3) As explained above, there are hidden complications in the plotting of titanian spinels on the same ratio plots used for Cr–Al–Fe^{3+}-spinels. In addition, cation ratio plots of the spinels from the several representative regions of the De Beers pipe show extensive overlap of values.

A new diagraming method was sought to fulfill essentially two purposes: (1) to show more clearly the compositional distinctions among the several kimberlite intrusions, in part by spreading out the data, and (2) to give a truer representation of fractionation and iron enrichment patterns. Cr *vs.* Fe^{2+} diagrams for the spinels were employed successfully. Their interpretation is in agreement with field evidence, in that it is inferred that three or four distinct intrusions occurred. Furthermore, it is clearer from the cation-cation plots than from the spinel ratio plots that all the intrusions probably tapped a single, fractionating magma source, and that the chronological order is as previously postulated (Pasteris, 1980).

Cr *vs.* Fe^{2+} diagrams for the spinels also suggest the nearly simultaneous injection of two kimberlite intrusives whose field relationships are unknown. The cation–cation diagrams, more clearly than their analogous cation ratio plots, provide insight into the relationship among Mg, Fe^{2+}, and Ti in the zoned spinels as well as highlight possible differences in fO_2 conditions during the several intrusions (Pasteris, 1980). Furthermore, spinel compositional trends which *are* evident on cation ratio plots are further enhanced by Cr *vs.* Fe^{2+} diagrams (see Figs. 1 and 2).

An unsuccessful attempt at interpreting Cr *vs.* Mg diagrams for the De Beers spinels underlines the importance of choosing the proper cations to plot. One must determine which compositional features are of interest (*e.g.*, differences between intrusions, differentiation trends), and how dependent the selected cations are upon compositional parameters not explicitly shown on the diagram. These two considerations reveal why Cr *vs.* Fe^{2+} plots are superior to Cr *vs.* Mg plots (Table 2) for kimberlitic spinels. In a particular facies of the De Beers kimberlite, the spinel compositions cluster at Fe^{2+}-values of about 0.35 and 0.75, an Fe^{2+}-range of 0.40. One might expect the same *range* on analogous Mg-plots, but comparable point clusters occur at 0.70 and 0.95, an Mg-range of only 0.25. The compressed appearance of the Mg-plots is accounted for by the fact that the high-Fe^{2+} spinels are

considerably richer in Ti than the low-Fe^{2+} ones. For the low-Fe^{2+} set of kimberlitic spinels, Ti ~ 0.3 and (1 + Ti) ~ ΣX^{2+} ~ 1.3; it follows that for Fe^{2+} = 0.35, Mg = 0.95. The high-Fe^{2+} group of spinels clusters at Ti ~ 0.45. For them, (1 + Ti) ~ ΣX^{2+} ~ 1.45; where Fe^{2+} = 0.75, then Mg = 0.70. The difference between the Mg values (0.95 and 0.70) thus is explained by the difference in Ti content between the two suites of spinels. The same effect accounts for a great deal of compression of data points for kimberlitic spinels at the high-Fe (*i.e.*, high-Ti) end of the FFM axis of ratio plots, as depicted in Table 2.

Summary

It is strongly suggested that geometric methods of projection be used in representing spinel compositions within the spinel prism, that only atomic ratios be plotted, and that Fe^{2+} and Fe^{3+} be represented separately, not as Fe_{total} (see Irvine, 1965; Haggerty, 1976, with substitution of the ratio 2Ti/2Ti+Al+Cr for Ti/Ti+Al+Cr). Petrologic interpretations of spinel data should account for the effect on cation ratios of the special stoichiometry of 2–4 (*e.g.*, titanian) spinels. Empirically chosen cation–cation plots for spinels may be helpful in distinguishing variations in melt composition. They are especially revealing in basalts and kimberlites with a strong Ti component in their spinels.

Acknowledgments

The study of kimberlitic spinels was carried out by the author as part of a Ph.D. thesis at Yale University. The author wishes to thank Drs. Stephen E. Haggerty and Nabil Z. Boctor for discussions on presently used methods of plotting spinel compositions and Drs. Gene C. Ulmer, Martin Engi, Alexandra Navrotsky, and an anonymous reviewer for their critical comments and suggestions on an early draft of the manuscript. However, she accepts full responsibility for all opinions expressed in this paper.

References

Arculus, R. J. (1974) Solid solution characteristics of spinels: pleonaste–chromite–magnetite compositions in some island-arc basalts. Carnegie Institution of Washington Year Book, 73, 322–327.

Boctor, N. Z. and Meyer, H. O. A. (1979) Oxide and sulfide minerals in kimberlites from Green Mountain, Colorado. In F. R. Boyd and H. O. A. Meyer, Eds., Kimberlites, Diatremes, and Diamonds, p. 217–228. American Geophysical Union, Washington, D. C.

Datta, R. K. and Roy, R. (1967) Equilibrium order–disorder in spinels. Journal of the American Ceramic Society, Ceramic Abstracts, 50, 578–583.

El Goresy, A. (1976) Oxide minerals in lunar rocks. In D. Rumble, Ed., Oxide Minerals, Chapter 5. Mineralogical Society of America, Washington, D. C.

Elthon, D. and Ridley, W. I. (1979) The oxide and silicate mineral chemistry of a kimberlite from the Premier Mine: Implications for the evolution of kimberlitic magmas. In F. R. Boyd and H. O. A. Meyer, Eds., Kimberlites, Diatremes, and Diamonds, p. 206–216. American Geophysical Union, Washington, D. C.

Evans, B. W. and Frost, B. R. (1975) Chrome-spinel in progressive metamorphism—a preliminary analysis. Geochimica et Cosmochimica Acta, 39, 959–972.

Haggerty, S. E. (1975) Chemistry and genesis of opaque minerals in kimberlites. Physics and Chemistry of the Earth, 9, 295–307.

Haggerty, S. E. (1976) Opaque mineral oxides in terrestrial igneous rocks. In D. Rumble, Ed., Oxide Minerals, Chapter 8. Mineralogical Society of America, Washington, D. C.

Haggerty, S. E. (1979) Spinels in high pressure regimes. In F. R. Boyd and H. O. A. Meyer, Eds., The Mantle Sample, p. 183–196. American Geophysical Union, Washington, D. C.

Irvine, T. N. (1965) Chromian spinel as a petrogenetic indicator. part I. theory. Canadian Journal of Earth Sciences, 2, 648–672.

Irvine, T. N. (1967) Chromian spinel as a petrogenetic indicator, part 2: petrologic applications. Canadian Journal of Earth Sciences, 4, 71–103.

Jackson, E. D. (1969) Chemical variation in coexisting chromite and olivine in chromite zones of the Stillwater Complex. Economic Geology Monograph 4, 41–71.

Mao, H. K. and Bell, P. M. (1974) Crystal-field effects in spinel: oxidation states of iron and chromium. Carnegie Institution of Washington Year Book, 73, 332–341.

Medaris, L. G. (1975) Coexisting spinel and silicates in alpine peridotites of the granulite facies. Geochimica et Cosmochimica Acta, 39, 947–958.

Mitchell, R. H. (1978a) Mineralogy of the Elwin Bay kimberlite Somerset Island, N. W. T., Canada. American Mineralogist, 63, 47–57.

Mitchell, R. H. (1978b) Composition of spinels in micaceous kimberlite from the Upper Canada Mine, Kirkland Lake, Ontario. Canadian Mineralogist, 16, 591–595.

Mitchell, R. H. (1979) Mineralogy of the Tunraq kimberlite, Somerset Island, N. W. T., Canada. In F. R. Boyd and H. O. A. Meyer, Eds., Kimberlites, Diatremes, and Diamonds, p. 161–171. American Geophysical Union, Washington, D. C.

Mitchell, R. H. and Meyer, H. O. A. (1980) Mineralogy of micaceous kimberlite from the Jos Dyke, Somerset Island, N. W. T. Canadian Mineralogist, 18, 241–250.

Muan, A., Hauck, J. and Lofall, T. (1972) Equilibrium studies with a bearing on lunar rocks. Proceedings of the Third Lunar Science Conference, 1, 185–196.

Pasteris, J. D. (1980) Opaque Oxide Phases of the De Beers Pipe Kimberlite (Kimberley, South Africa) and Their Petrologic Significance. Ph.D. Thesis, Yale University, New Haven.

Rawson, S. A., and Irvine, T. N. (1980) Mg–Fe^{2+} partitioning between olivine and ferrian ulvospinel. Carnegie Institution of Washington Year Book, 79, 332–337.

Ridley, W. I. (1977) Crystallization trends of spinels in Tertiary basalts from Rhum and Muck and their petrogenetic signifi-

cance. Contributions to Mineralogy and Petrology, 64, 243–255.

Roeder, P. L., Campbell, I. S. E., and Jamieson, H. E. (1979) A re-evaluation of the olivine-spinel geothermometer. Contributions to Mineralogy and Petrology, 68, 325–334.

Stevens, R. E. (1944) Composition of some chromites of the Western Hemisphere. American Mineralogist, 29, 1–34.

Manuscript received, February 20, 1981;
accepted for publication, October 29, 1981.